Computational insights into function and inhibition of fatty acid amide hydrolase

ARTICLE *in* EUROPEAN JOURNAL OF MEDICINAL CHEMISTRY · SEPTEMBER 2014

Impact Factor: 3.45 · DOI: 10.1016/j.ejmech.2014.09.037 · Source: PubMed

4 AUTHORS:

Giulia Palermo
École Polytechnique Fédérale de Lausanne
15 PUBLICATIONS **71** CITATIONS
SEE PROFILE

Ursula Rothlisberger
École Polytechnique Fédérale de Lausanne
291 PUBLICATIONS **8,340** CITATIONS
SEE PROFILE

Andrea Cavalli
University of Bologna
171 PUBLICATIONS **4,914** CITATIONS
SEE PROFILE

Marco De Vivo
Istituto Italiano di Tecnologia
43 PUBLICATIONS **713** CITATIONS
SEE PROFILE

European Journal of Medicinal Chemistry xxx (2014) 1–12

Contents lists available at ScienceDirect

European Journal of Medicinal Chemistry

journal homepage: http://www.elsevier.com/locate/ejmech

Computational insights into function and inhibition of fatty acid amide hydrolase

Giulia Palermo [a, b], Ursula Rothlisberger [b], Andrea Cavalli [a, c], Marco De Vivo [a, *]

[a] Department of Drug Discovery and Development, Italian Institute of Technology, Via Morego 30, 16163 Genova, Italy
[b] Laboratory of Computational Chemistry and Biochemistry, Institute of Chemical Sciences and Engineering, École Polytechnique Fédérale de Lausanne (EPFL), CH-1015 Lausanne, Switzerland
[c] Department of Pharmacy and Biotechnology, University of Bologna, Via Belmeloro 6, I-40126 Bologna, Italy

ARTICLE INFO

Article history:
Received 20 June 2014
Received in revised form
1 September 2014
Accepted 11 September 2014
Available online xxx

Keywords:
FAAH
Molecular dynamics
QM/MM

ABSTRACT

The Fatty Acid Amide Hydrolase (FAAH) enzyme is a membrane-bound serine hydrolase responsible for the deactivating hydrolysis of a family of naturally occurring fatty acid amides. FAAH is a critical enzyme of the endocannabinoid system, being mainly responsible for regulating the level of its main cannabinoid substrate anandamide. For this reason, pharmacological inhibition of FAAH, which increases the level of endogenous anandamide, is a promising strategy to cure a variety of diseases including pain, inflammation, and cancer.

Much structural, mutagenesis, and kinetic data on FAAH has been generated over the last couple of decades. This has prompted several informative computational investigations to elucidate, at the atomic-level, mechanistic details on catalysis and inhibition of this pharmaceutically relevant enzyme. Here, we review how these computational studies – based on classical molecular dynamics, full quantum mechanics, and hybrid QM/MM methods – have clarified the binding and reactivity of some relevant substrates and inhibitors of FAAH. We also discuss the experimental implications of these computational insights, which have provided a thoughtful elucidation of the complex physical and chemical steps of the enzymatic mechanism of FAAH. Finally, we discuss how computations have been helpful for building structure–activity relationships of potent FAAH inhibitors.

1. Introduction

Fatty acid amide hydrolase (FAAH – Fig. 1) [1–3] is a membrane-bound serine hydrolase that was initially identified as hydrolyzing the biologically active lipid oleamide (**1** – Scheme 1) [4]. However, it was later demonstrated that FAAH cleaves several other fatty acids, with remarkable preference for the endogenous cannabinoid anandamide [*N*-arachidonoyl-ethanolamine (**2**) – Scheme 1], a naturally occurring fatty acid agonist of cannabinoid receptors [2,3,5–9]. Therefore, inhibition of FAAH activity amplifies and extends the biopharmacological effects of these lipid-derived messengers, including the satiety factor oleoylethanolamide [10,11] and the anti-inflammatory/analgesic agent palmitoylethanolamide [12].

Pharmacological inhibition of FAAH allows modulation of the endogenous levels of cannabinoids. It is thus a promising drug target to treat pain, inflammation, and several other diseases, including cancer. Pharmacological inhibition of FAAH could also solve the main problems of therapeutic agents that act as direct agonists of the cannabinoid receptor CB1, which often cause severe side effects such as dysphoria and negative effects on motility, memory, and sleep [13]. In this regard, FAAH knockout ($FAAH^{-/-}$) mice show substantially increased levels of anandamide in the brain and reduced pain sensation without observable hypomotility, hypothermia, or catalepsy [14–19]. Thus, over the last decade, both academic and industrial groups have started drug discovery programs targeting FAAH. This has prompted computational studies on this enzyme with the common aim of deciphering, at the atomic level, both enzymatic function and inhibition.

Here, we review several informative computational studies on FAAH, including our own recent work. Overall, we aim to show how classical and first-principles-based computations have helped addressing relevant questions on the function and inhibition of FAAH in relation to the available experimental data on FAAH. We will examine the main structural features and energetics for ligand binding and hydrolysis during FAAH catalysis, as well as key

* Corresponding author.
E-mail address: marco.devivo@iit.it (M. De Vivo).

http://dx.doi.org/10.1016/j.ejmech.2014.09.037
0223-5234/

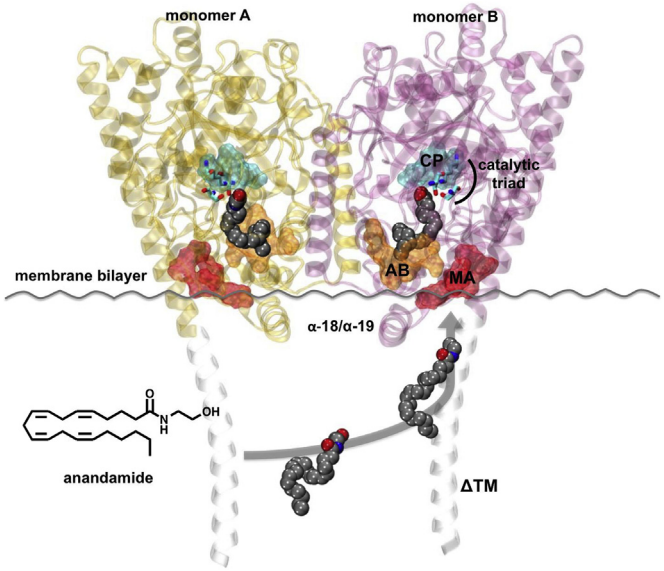

Fig. 1. Overview of the FAAH protein (pdb 1MT5) [1] in complex with anandamide (chemical structure at the bottom left) [119]. The enzyme is a membrane protein composed of two subunits, which are the monomers A (yellow ribbons) and B (magenta ribbons). The protein is inserted in the membrane thanks to the α-18 (residues 410–426) and α-19 (residues 429–438) transversal helices and the deleted transmembrane (ΔTM) domain (residues 9–29, shown as transparent ribbons). The membrane bilayer is indicated with a gray line. Anandamide (gray, in space-filling representation) is thought to reach the catalytic site via a "membrane access" channel (MA – shown in red molecular surface). An adjacent "acyl-chain binding" channel (AB – orange), which in the crystal structure is occupied by the arachidonoyl chain of the bound methyl arachidonyl fluorophosphonate (MAFP), likely contributes to the proper accommodation of the substrate during catalysis. At the top of the catalytic region, a third channel (cyan) constitutes the "cytosolic port" (CP) that allows the exit of the leaving group after hydrolysis. The Ser241-Ser217-Lys142 catalytic triad is indicated with cyan sticks. (For interpretation of the references to color in this figure legend, the reader is referred to the web version of this article.)

pharmacophoric elements for covalent inhibition of FAAH, as elucidated by several computational studies. Finally, we mention aspects related to FAAH catalysis and lipid selection that are still unclear and that could be the subject of future computational investigations.

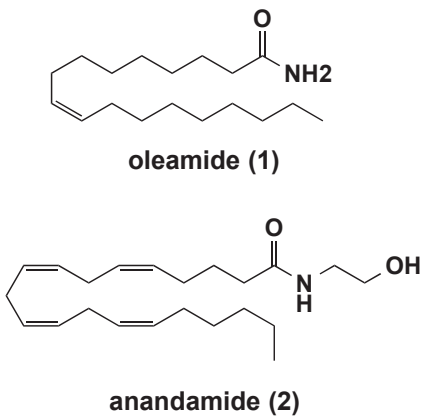

Scheme 1. Chemical structure of oleamide (**1**) and anadamide [*N*-arachidonoyl-ethanolamine (**2**)] [4,6].

1.1. FAAH structure

FAAH is a 65 kD protein that was purified in 1996 by Cravatt et al. from rat liver membranes (*r*FAAH – Fig. 1) [2]. Based on sequence analysis, FAAH belongs to the amidase signature (AS) enzyme family. Unlike most AS enzymes, FAAH is an integral membrane protein with a transmembrane (TM) domain (amino acids 9–29). When expressed with deletion of the predicted TM domain (as TM-domain-deleted FAAH – ΔTM-FAAH), *r*FAAH maintains the wild-type protein's association with membranes as well as its enzymatic properties [20]. These results indicate that FAAH possesses multiple domains for membrane association, which were subsequently identified as the α-18/α-19 transversal helices [1].

The first X-ray crystal structure of the *r*FAAH was determined for ΔTM *r*FAAH in complex with an analogue of anandamide, the irreversible inhibitor methyl arachidonyl fluorophosphonate (MAFP) at 2.8 Å resolution (PDB code: 1MT5) [1]. This structure revealed a dimeric protein with a characteristic core structure of a twisted β-sheet surrounded by 24 α-helices. Interestingly, the crystal structure also revealed multiple pockets to the catalytic site of FAAH (Fig. 1). These cavities are the "membrane access" (MA) channel, located in proximity to the α-18/α-19 helices, which connects the membrane surface to the core of the FAAH active site. The substrate is thought to reach the catalytic site via this MA channel, reaching the hydrolytic Ser241–Ser217–Lys142 catalytic triad. The adjacent "acyl-chain binding" (AB) channel – found to be occupied by the arachidonyl chain of the bound MAPF [1] – likely provides an extra space for substrate binding. A cytosolic port (CP) is located at the top of the active site where it provides an exit route for the leaving group, after substrate hydrolysis, toward the cytosol.

Given the multiple membrane association possibilities of FAAH, protein expression and purification have been challenging for the human isoform (*h*FAAH) that shares ~82% sequence identity with *r*FAAH [21]. For this reason, a '*humanized*' rat FAAH (*h*/*r*FAAH) was resolved at 2.75 Å (PDB code: 2VYA) in complex with the piperidine-based inhibitor PF-750. In this structure, six amino acids of the active site were mutated into those of the human FAAH protein sequence (namely, Leu192Phe, Phe194Tyr, Ala377Trp, Ser435Asn, Ile491Val, and Val495Met) [21]. The *h*/*r*FAAH structure showed similar structural features as *r*FAAH. One remarkable difference, however, was detected at the interface between the AB and MA pockets, where a key residue (Phe432) was rotated by about 80° along the Cα–Cβ axis, due to the presence PF-750 in the *h*/*r*FAAH structure (Fig. 2). Thus, the MA channel of *h*/*r*FAAH in presence of PF-750 was remarkably larger than in *r*FAAH. This led to the suggestion that Phe432 might act as a "*dynamic paddle*" that directs the FAAH substrate into pre-active conformations for hydrolysis, located in either AB or MA during catalysis. Following the first *h*/*r*FAAH structure, several additional *h*/*r*FAAH structures bound with different covalent inhibitors were determined, confirming the marked structural flexibility of Phe432 [21–26].

1.2. Experimental findings on function and inhibition of FAAH

The mechanistic details of FAAH reactivity were extensively characterized by structural [1,21–26] and mutational [27] studies, further supported via several informative theoretical investigations, as discussed later in this review [28–32]. The hydrolytic function of FAAH is performed by an unusual Ser241–Ser217–Lys142 catalytic triad, which replaces the typical Ser–His–Asp motif of the serine hydrolases [1]. The enzymatic reaction comprises two main chemical steps (Scheme 2), which are the enzyme acylation (**A** → **D**) and subsequent deacylation (**D** → **E**), with release of the final product. During the enzyme

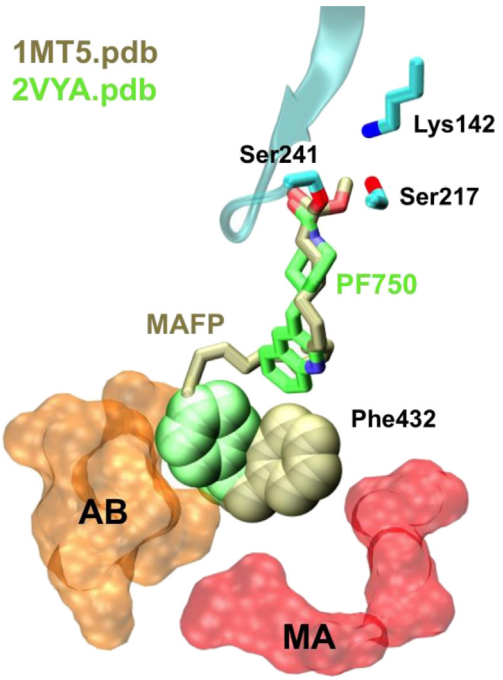

Fig. 2. Superimposition of the crystal structures of the *rat* FAAH covalently bound to the methyl arachidonyl fluorophosphonate (MAFP – 1MT5.pdb, solved at 2.8 Å resolution) [1] and of the *h/r* FAAH in complex with the piperazine-based inhibitor PF-750 (2VYA.pdb, solved at 2.75 Å resolution) [21]. The covalently bound MAFP (tan) and PF-750 (green) inhibitors, as well as the catalytic Ser241-Ser217-Lys142 residues (cyan) are shown in sticks. The two structures share a similar active site with one remarkable difference at the interface between the "membrane access" (MA) and "acyl-chain binding" (AB) channels, given by the rotation of the interface residue Phe432 (shown in space-filling representation). In the presence of the MAFP inhibitor, Phe432 (tan) allows the location of the inhibitor arachidonoyl chain within the AB channel. When in complex with the PF-750 inhibitor, Phe432 (green) rotates the Cα–Cβ dihedral of ~80°, thereby opening the MA channel, which is remarkably larger. (For interpretation of the references to color in this figure legend, the reader is referred to the web version of this article.)

acylation, the deprotonated Lys142 activates the Ser241 nucleophile via a "proton shuttle" mechanism that involves Ser217. Once deprotonated, the activated Ser241 attacks the carbonyl group of the substrate with the consequent formation of a tetrahedral intermediate. Then, a reversed proton transfer, from Lys142 through Ser217, leads to protonation of the leaving group and subsequent formation of the acyl-enzyme adduct. Mutagenesis and theoretical studies have indeed supported an enzymatic mechanism in which Lys142 acts as a general base in the acylation step of the catalytic process [27]. After this first chemical step, the enzyme deacylation terminates the catalytic cycle, with the attack of a water molecule on the carbonyl group of the acyl–enzyme adduct. The deprotonation of the nucleophilic water, through a further proton transfer involving the catalytic triad, allows the formation and subsequent release of the final product. The restoration of the initial protonation state of the catalytic triad closes the catalytic loop.

The formation of a stable acyl-enzyme adduct along this enzymatic mechanism has been corroborated, over the years, by the discovery of covalent inhibitors of FAAH [33]. These compounds can form a covalent bond with the nucleophilic Ser241, thereby blocking the catalytic function of FAAH as long as the inhibitor remains irreversibly bound to the enzymatic pocket, after enzyme acylation [33]. In this regard, a first generation of FAAH inhibitors was discovered using the natural substrates of FAAH as a template. This generated, for example, the anandamide analog MAFP (**3** – Scheme 3) inhibitor and the trifluoromethyl ketones. These inhibitors, however, were not selective, inhibiting several other serine hydrolases too. Later, several reversible inhibitors were discovered, including new trifluoromethyl ketones, α-ketoesters, α-ketoamides, and the α-ketoheterocycles, including the highly selective OL135 (**4** – Scheme 3) [34]. Very recently, a new series of α-ketoheterocycles compounds, as derivatives of OL135 (for example, compound **5** – Scheme 3), have been described as irreversibly targeting a cysteine in the FAAH catalytic site (Cys269) of the enzymatic cavity, while also forming a reversible covalent bond with Ser241 [17]. Potent irreversible inhibitors were also developed, showing a promising drug-like profile [33]. Of the irreversible inhibitor compound classes, we mention here the compound class

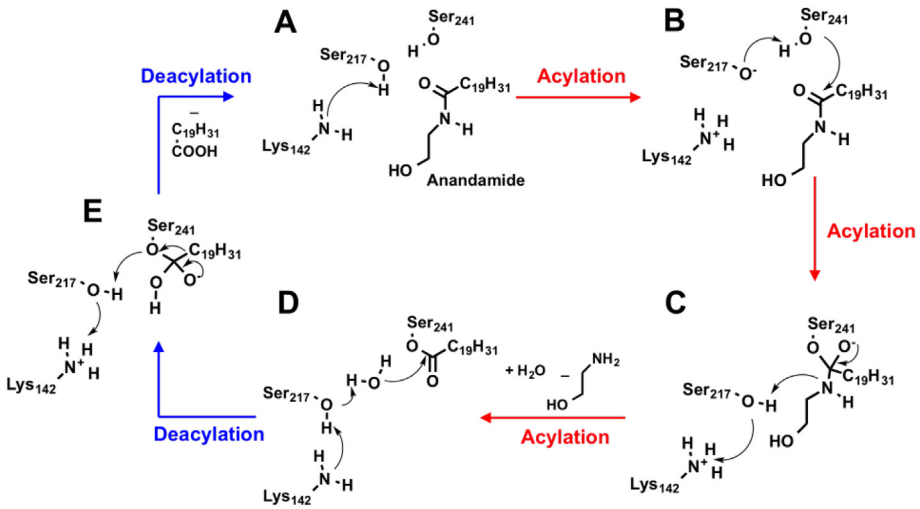

Scheme 2. FAAH catalytic cycle, shown for the anandamide substrate [27]. The catalytic mechanism has two main steps: acylation step (**A** → **D**, highlighted with red arrows) and deacylation step (**D** → **E**, highlighted with blue arrows). During the enzyme acylation (**A** → **D**), the Lys142 base activates the Ser241 nucleophile via a "proton shuttle" mechanism that involves Ser217 (**A**). The activated Ser241 attacks the carbonyl group of the substrate (**B**) with the formation of a tetrahedral intermediate (**C**). A second proton transfer involving Ser217 and Lys142 leads to the collapse of the tetrahedral intermediate with the exit of ethanolamine as a substrate leaving group (**D**). The enzyme deacylation (**D** → **E**) terminates the catalytic cycle with the attack of a water molecule on the acyl-enzyme adduct (**D**) and the consequent formation of a tetrahedral intermediate (**E**). The release of arachidonic acid as a final product of the anandamide hydrolysis leads to the restoration of the initial protonation state and ordered H-bond network of the catalytic triad (**A**). (For interpretation of the references to colour in this figure legend, the reader is referred to the web version of this article.)

Please cite this article in press as: G. Palermo, et al., Computational insights into function and inhibition of fatty acid amide hydrolase, European Journal of Medicinal Chemistry (2014), http://dx.doi.org/10.1016/j.ejmech.2014.09.037

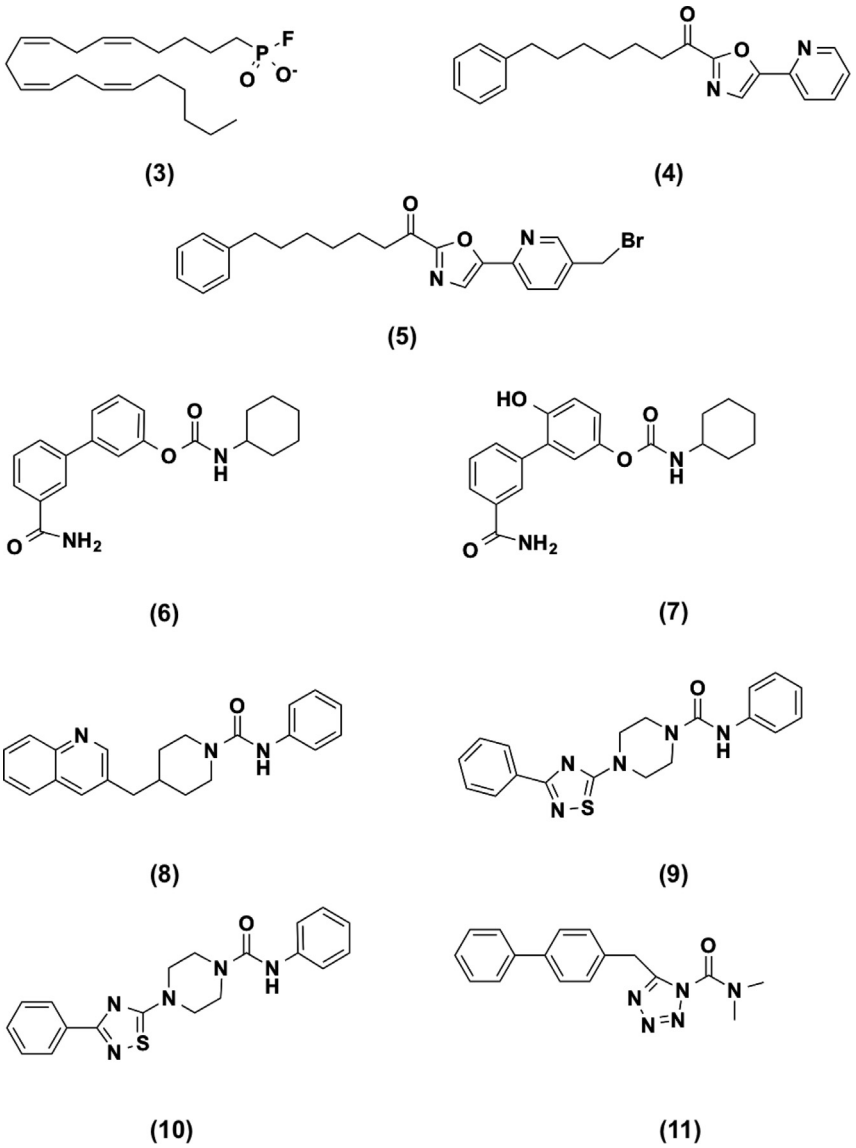

Scheme 3. Chemical structure of the methyl arachidonyl fluorophosphonate [MAFP – (**3**)] [33], the α-ketoheterocycle OL135 (**4**) [33,34] and its recent analogue (**5**) [17], the carbamate-based compounds URB597 (**6**) [37] and URB937 (**7**) [38], the urea-based compounds PF-750 (**8**) [42], PF-622 (**9**) [42], JNJ1661010 (**10**) [41] and LY2183240 (**11**) [33].

characterized by a carbamic moiety substituted with alkyl or aryl groups at their O– and N– termini [35,36]. URB524 is the most potent of this first series of carbamate-based inhibitors (IC_{50} = 63 nM). It then generated the more potent URB597 (**6** – Scheme 3 – IC_{50} = 4.6 nM) [37]. Recently, a brain-impenetrant member of this class of compounds was disclosed [URB937 (**7** – Scheme 3 – IC_{50} = 26.8 nM)], with substantial analgesic effects in animal models [38].

Crystallographic studies have shown that carbamate-based inhibitors act via the carbamoylation of the nucleophilic Ser241 of FAAH, blocking the enzymatic function through covalent inhibition [25]. This mechanism of inhibition was also described by both crystallographic and theoretical studies, which confirmed the formation of a covalent bond between the hydrolyzed inhibitor and Ser241 [39,40]. More recently, a newer class of FAAH inhibitors was discovered, in which the carbamic group was replaced by the urea functionality [33]. Interestingly, compounds bearing a cyclic piperidine/piperazine urea scaffold, such as PF-750 (**8** – Scheme 3 – IC_{50} = 16.2 nM), PF-622 (**9** – Scheme 3 – IC_{50} = 33.0 nM) and urea JNJ1661010 (**10** – Scheme 3 – IC_{50} = 33 nM) [41], show a covalent inhibition of FAAH, similar to the one observed for carbamates, with improved selectivity [42]. However, there are cases in which urea-based compounds show lower selectivity. One example is the potent heterocyclic urea compound LY2183240 (**11** – Scheme 3 – IC_{50} = 12.4 nM) [33].

Despite these structural, chemical, and biochemical data, there remain relevant open questions on the mechanism of function and inhibition of FAAH. The mechanistic details for hydrolysis of some endogenous substrates and inhibitors have been well clarified by informative computational studies discussed hereafter. But the proper location of anandamide within the intricate FAAH catalytic site in the reactant state, for example, is still unclear [1,43]. In this regard, we will review our recent classical molecular dynamics (MD) investigation on anandamide bound to FAAH. It points to structural flexibility as playing a key role in the efficient formation of catalytically relevant conformations – i.e. conformations more prone to undergo hydrolysis – of the substrate bound to FAAH. In particular, this will be discussed in the context of crucial factors that

Please cite this article in press as: G. Palermo, et al., Computational insights into function and inhibition of fatty acid amide hydrolase, European Journal of Medicinal Chemistry (2014), http://dx.doi.org/10.1016/j.ejmech.2014.09.037

regulate substrate selectivity and, likely, lipid degradation, as suggested by a variety of experimental evidence [21,23–26,44,45]. Then, we will focus on a second work of ours, which clarifies the mechanism of FAAH inhibition by new and potent piperidine/piperazine urea-based inhibitors. In this case, we will demonstrate how classical MD and quantum mechanics (QM) have been used, over the last few years, to dissect the mechanism of covalent inhibition of potent FAAH inhibitors, thus providing hints for the rational design of new and more specific FAAH inhibitors.

2. Computational methods

The overall computational work reviewed here is based on classical MD simulations, full QM, and hybrid quantum mechanics/molecular mechanics (QM/MM) calculations. Before discussing the computational findings on FAAH catalysis and inhibition, we briefly introduce the basic concepts and vocabulary of these methods. This meant to provide a minimal theoretical basis, while the interested reader is encouraged to delve into the many review articles and books that focus on the theoretical background of these computational methods [40,48–112].

2.1. Quantum mechanics (QM)

Methods based on QM aim at the direct solution of the Schrödinger equation and are therefore considered the most accurate and reliable methods. QM approaches can be classified as *ab initio*, density functional theory (DFT), or semiempirical schemes. Given the difficulty of finding the exact solution for the Schrödinger equation, approximate methods must be used for many-electron systems. The simplest approximation is the Hartree–Fock (HF) method, in which the many-electron wave function is reduced to an antisymmetric product of one-electron wave functions (a single Slater determinant). HF accounts for exchange effects, while it fails to recognize that electronic motions are correlated, therefore neglecting electron correlation effects. More sophisticated methods can improve the HF approximation, such as Møller–Plesset (MP) perturbation theory [46] in which electron correlation is described as a perturbation to the HF solution. Second order Møller–Plesset (MP2) calculations are quite standard, while the computational cost increases considerably if higher orders of perturbation are used.

In contrast, DFT is based on the central idea proposed by a theorem of Hohenberg and Kohn [47] in 1964, which states that the ground-state energy of a system of interacting electrons is a unique functional of its electron density. One year later, Kohn and Sham proposed a way to determine the electron density [48] for a system with interacting electrons. The KS approach proposed a functional for the energy where the so-called exchange-correlation energy functional is the only unknown term. Therefore, the major task within the DFT framework is the modeling of exchange and correlation interactions for which an explicit analytical formula is not known. Thus, the quality of the exchange-correlation functional heavily affects the quality of the prediction by DFT calculations. Several different approximations are used, of which the most basic is the local density approximation (LDA). Later, improved approximations include generalized gradient approximations (GGA), which has generated several gradient-dependent parameterizations for the exchange-correlation energy functional. Among the most common gradient-corrected functionals, we mention the Becke exchange functional, and the Lee, Yang, and Parr correlation functional, commonly abbreviated as the BLYP exchange-correlation functional [49,50]. We also mention the hybrid B3LYP functional [51], which uses a mixture of exact exchange with the Becke functional [49], the LYP functional [50], the VWN functional [52], and three empirical parameters. It is worth mentioning that calculations at the DFT/B3LYP level of theory are rather common nowadays in quantum chemistry, and are also used more and more to study biological systems [53,54]. Recent advances have led to the development of the so-called *Minnesota functionals* by D. Truhlar [55], including the meta-hybrid M06[56] functional. This includes terms that depend on the kinetic energy density with 27% of exact exchange. As a final example of a remarkable advance in QM-based methods, we mention the seminal work of Car and Parrinello, who proposed in 1985 a new method of performing DFT-based molecular dynamics [57] (the so-called Car-Parrinello MD method), which allows first-principles-based simulations of (biological) systems to be run, explicitly including entropic effects. Over the last couple of decades, the Car-Parrinello method has also been successfully applied to a number of pharmaceutically relevant targets [58–62].

Semiempirical methods are simplified versions of *ab initio* and DFT methods, in which computationally demanding integrals are approximated or neglected in order to speed up calculations. The approximations make use of experimental data. Standard semiempirical methods are MNDO [63], AM1 [64], PM3[64] and the improved semiempirical method PDDG/PM3 [66]. These are parameterized primarily with respect to ground–state properties, with particular emphasis on the energies and geometries of organic molecules. The low computational cost of these semiempirical methods is counterbalanced by their limited accuracy, which depends on the type of parameterization and empirical corrections.

2.2. Molecular dynamics (MD)

This method allows the solution of the classical equation of motion for a set of particles to describe the time-evolution of a system at finite temperature. The result is a trajectory representing the computed configurations of the molecular system as a function of time. This trajectory provides insight into the dynamic and thermodynamic properties of the system under investigation. The method was first developed more than 50 years ago [67–69] and, given its success in describing diverse biological problems, it is in continuous development [70,71].

In classical MD, the potential energy of the system is determined by an empirical force field (FF) that is parameterized to reproduce experimental or *ab-initio* data. The FF is defined as the sum of different contributions mimicking the molecular binding mediated by the electrons, and it is usually composed of bonded terms describing stretching, bending, and torsional vibrational modes, in addition to non-bonded interactions describing dispersion and electrostatic forces Eq. (1)):

$$V = \sum_{\text{bonds}} K_R(\mathbf{R}-\mathbf{R}_{eq})^2 + \sum_{\text{angles}} K_\theta(\theta-\theta_{eq})^2 + \sum_{\text{diherals}} \frac{V_n}{2}[1 + \cos(n\phi-\gamma)] + \sum_{i<j}\left[\frac{A_{ij}}{\mathbf{R}_{ij}^{12}} - \frac{B_{ij}}{\mathbf{R}_{ij}^{6}} + \frac{q_i q_j}{\in \mathbf{R}_{ij}}\right] \quad (1)$$

To date, the most common force fields are OPLS [72], AMBER [73], GROMOS [74] and CHARMM [75], which are broadly used to study biomolecular systems. Apart from the potentials developed for biological macromolecules, it is worth mentioning that computational drug design and drug discovery studies also profit from both the Generalized AMBER Force Field (GAFF) [76] and CHARMM General Force Field (CgFF) [77] developed for small organic compounds. For example, the relatively cheap computational cost of these force fields allows for fast screening of large libraries of chemical compounds [78,79]. Moreover, molecular dynamics simulations when coupled to enhanced sampling techniques such as metadynamics [80,81] or free-energy perturbation

Please cite this article in press as: G. Palermo, et al., Computational insights into function and inhibition of fatty acid amide hydrolase, European Journal of Medicinal Chemistry (2014), http://dx.doi.org/10.1016/j.ejmech.2014.09.037

[82,83], can be efficiently employed for free energy calculations and lead optimization [84].

2.3. Quantum mechanics/molecular mechanics (QM/MM)

QM and force-field-based molecular mechanics (MM) methods can be combined, forming the so-called QM/MM approach. Originally proposed in 1976 by Warshel and Levitt for studying the enzymatic reaction in lysozyme [85], many different QM/MM implementations have been generated in recent decades, being efficaciously used to investigate questions related to both biology and material science [40,86–91]. Common hybrid QM/MM schemes are the ONIOM [92] method included in the GAUSSIAN suite of programs [93], or the hybrid Hamiltonian approaches included in CPMD [94,95] and CP2K [96]. QM/MM methods are motivated by the fact that a model system of a protein immersed in explicit solvent can easily reach a size of 100,000 atoms or more, while only a few hundred atoms, at most, can be described at the QM level. In QM/MM studies of enzymatic catalysis, for example, the region of interest of the model system (the enzyme's binding pocket and the ligand) is treated at a higher level of accuracy (QM level), while the remainder of the system is treated at the MM level of theory (a representative QM/MM partitioning of a biological system – e.g. FAAH – is shown in Fig. 3). The QM region can be described at several different levels of theory, spanning from semiempirical to *ab-initio* or DFT. Since its first appearance [85], QM/MM approaches have been successfully applied to a growing number of drug design-related studies [97–102] and enzymatic mechanisms [88,102–107]. Importantly, the continued development in the field has allowed researchers to study the reactivity of biological systems of increasing size (up to 200,000 atoms) and complexity [107]. We are currently carrying out Car-Parrinello QM/MM simulations of FAAH embedded in an atomistic membrane/water environment (Fig. 3) with the aim to investigate the enzymatic reactivity taking into account a realistic biological environment. More recently, these hybrid methods have been integrated into docking calculations [108–110] and used for computing the binding affinity of drugs [109,111,112], suggesting QM/MM as a useful tool for *in silico* drug design and lead optimization.

In fact, 2013 Nobel Prize in Chemistry was given in recognition of the seminal contributions of Karplus, Levitt, and Warshel in developing multiscale models for complex chemical systems. The QM/MM scheme was specifically mentioned in honoring the groundbreaking work of the Nobel accolades in the field of molecular simulations.

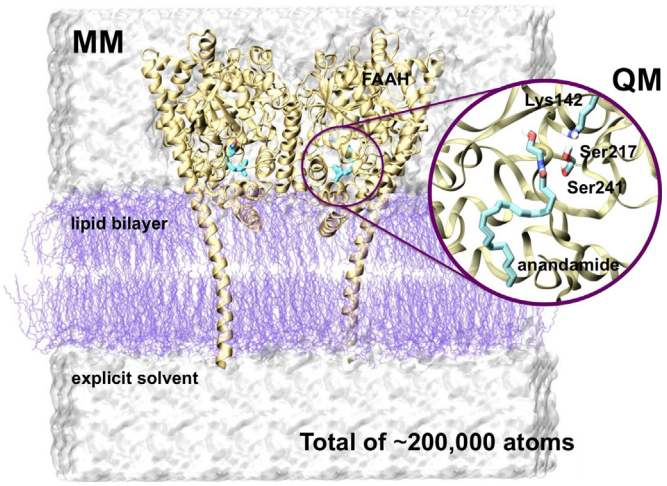

Fig. 3. Representative QM/MM partitioning of a biological system (shown for the *rat* FAAH in complex with anandamide embedded in a realistic membrane/water environment). While the enzyme (gold), the solvent (gray surface), and the lipid bilayer (violet) are treated at the MM level of theory, only the atoms directly involved in the reactive process (shown as cyan sticks) are treated at the QM level. The box on the right is a close view of the reactive region of the complex, where anandamide and part of the catalytic triad residues Ser241, Ser217 and Lys142 (81 atoms in total) are treated at the QM level. A total of ~200,000 atoms are explicitly considered. This representative picture has been adapted from our study on FAAH catalysis [119] (For interpretation of the references to color in this figure legend, the reader is referred to the web version of this article.)

3. Computational investigations of the enzyme FAAH

3.1. Enzymatic mechanism of FAAH

In 2002, the first X-ray structure of FAAH in complex with an anandamide analogue, i.e. the irreversible inhibitor methyl arachidonyl fluorophosphonate (MAFP), prompted several computational investigations on both FAAH catalysis and inhibition. Much credit for important computational insights is due to the groups of Jorgensen [28,32,113] and Mulholland [29–31,39,40,114,115], who have independently modeled the acylation step of the enzymatic catalysis (**A** → **D** in Scheme 2) using different computational approaches.

First, Mulholland's group modeled the proton transfer and acylation step that leads to the tetrahedral intermediate (**A** → **C**) for the oleamide substrate, using QM/MM in an adiabatic mapping approach [29]. Semiempirical PM3^{64}/CHARMM [75] calculations, further corrected via Density Functional Theory (DFT) B3LYP [51]/6-31 + G(d)//PM3-CHARMM, indicated that the two proton transfers needed for enzyme acylation are concerted. The calculated barrier at the PM3^{64}/CHARMM [75] was 36.0 kcal mol^{-1}, corrected via DFT to 18.0 kcal mol^{-1}. These findings are consistent with the experimental value related to the overall catalytic rate (k_{cat} = 14.4 ± 0.63 s^{-1}) [27] that, employing transition state theory and assuming a transmission factor of unity, results in an activation barrier of the rate-limiting step of ~16 kcal mol^{-1}. Subsequently, they investigated the hydrolysis of the tetrahedral intermediate to complete the acylation step (i.e., looking at **A** → **D**) for oleamide, using the same approach, with calculations at the PM3^{64}/CHARMM [75] level of theory. The obtained energy profile indicated a small difference between the calculated barriers for **A** → **C** and **C** → **D** reactions (i.e., **A** → **C** = 36.0 kcal mol^{-1}; **C** → **D** = 40.0 kcal mol^{-1}). This proposed mechanism was corroborated with a study by Jorgensen et al. [32], who investigated the overall acylation process via free energy perturbation (FEP) calculations, using Monte Carlo (MC) simulations in combination with PDDG/PM3. The calculated energy barrier for the formation of the tetrahedral intermediate (**A** → **C**, 32.4 kcal mol^{-1}) was found to be comparable with the result obtained by Mulholland et al. (36.0 kcal mol^{-1}), whereas the barrier for the collapse of the tetrahedral intermediate (**C** → **D**) was 15.8 kcal mol^{-1}, indicating the formation of tetrahedral intermediate as the rate-limiting step. Interestingly, both Mulholland's and Jorgensen's studies confirm that semiempirical methods often overestimate the energetic barriers [116]. Nevertheless, the agreement of the results obtained by the two research groups strongly corroborates the mechanistic conclusions of a "*striking multi-step sequence of events*" for this chemical process [117], providing an excellent atomic-level description for the first acylation step of oleamide hydrolysis in FAAH.

The acylation process for the methyl oleate was also studied in order to investigate the experimental evidence that FAAH cleaves amides slightly faster than esters [27]. In this case, Mulholland et al. obtained a similar energy profile for the substrate methyl oleate, compared to that found for oleamide, with a concerted process characterized by concomitant proton transfers and nucleophilic

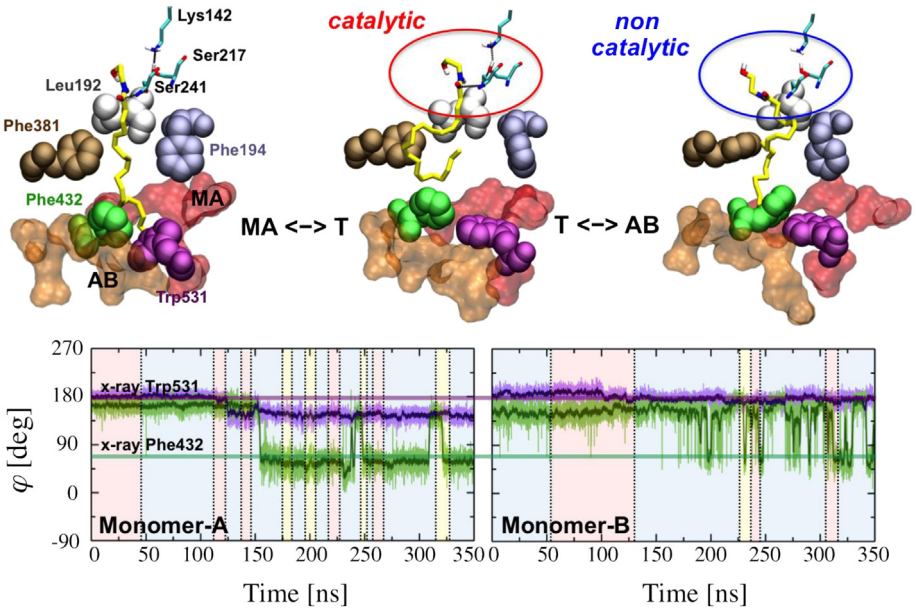

Fig. 4. Upper panel: Selected snapshots from MD simulations showing the MA ↔ AB transitions of anandamide within the *rat* FAAH active site [1]. The MA (red) and AB (orange) channels are shown in molecular surface, while anandamide is shown in yellow sticks. Key residues are in space-filling representation, namely, Leu192 (gray), Phe194 (ice blue), Phe381 (maroon), Phe432 (green), and Trp531 (violet). The Ser241-Ser217-Lys142 catalytic triad is shown in cyan sticks. Catalytically relevant conformations of anandamide, which are prone to undergo nucleophilic attack by the nucleophilic Ser241, are mainly sampled when the flexible arachidonoyl tail is located at the MA/AB interface (central panel), while the location of the substrate acyl chain in the AB cavity (right panel) leads to non-catalytic conformations of the complex. Lower panel: Time evolution of the anandamide acyl chain location, from ~350 ns of μs MD simulations of the *rat* FAAH/anandamide complex in a membrane/water atomistic framework [119]. The background is in red when anandamide is located in MA, in yellow when in AB, and in cyan at the MA/AB interface. The time evolution of the dihedral angle φ along the Cα–Cβ of the key Phe432 (green) and Trp531 (violet) is also reported for both FAAH monomers, indicating that a concerted conformational change of these residues triggers the MA ↔ AB transitions of anandamide. Averages are shown in solid lines. The thick bars indicate the values of the φ angle for Phe432 (φ ~ 65°) and Trp531 (φ ~ 180°) in the X-ray structure [1]. Angles are expressed in degrees. (For interpretation of the references to color in this figure legend, the reader is referred to the web version of this article.)

attack for enzyme acylation [115]. The energetic barriers for the formation (**A** → **C**) and the collapse (**C** → **D**) of the tetrahedral intermediate for methyl oleate hydrolysis were found to be 44.0 kcal mol^{-1} and 47.0 kcal mol^{-1}, respectively. These calculations confirm the formation of the tetrahedral intermediate as rate-limiting for the acylation process, as observed for the substrate oleamide (where **A** → **C** = 36.0 kcal mol^{-1}; **C** → **D** = 40.0 kcal mol^{-1}). Moreover, the lower rate-limiting energy barrier for oleamide, with respect to methyl oleate, confirmed that FAAH prefers to hydrolyze amides [27].

To clarify the essential role of the Lys142 residue in initiating the overall catalytic process, Jorgensen et al. studied the first acylation step for oleamide and methyl oleate introducing the Lys142Ala mutation [32]. The FAAH preferential hydrolysis of amides with respect to esters is reverted in the Lys142Ala FAAH mutant [27]. Since Ala142 is not able to accept protons, the authors proposed an alternative mechanism. In detail, the acylation occurs in a concerted mechanism in which Ser217 deprotonates Ser241 for the nucleophilic attack, which occurs simultaneously with the protonation of the leaving group by the former. As a result, the computed barriers for oleamide and methyl oleate were 40.1 kcal mol^{-1} and 35.2 kcal mol^{-1}, respectively, indicating preferential hydrolysis of esters in the Lys142Ala FAAH mutant.

Regarding the acylation step, Mulholland et al. emphasized that one key aspect of the FAAH catalytic machinery is the pyramidal inversion of the substrate nitrogen, which is occurring during the enzyme acylation [114,115]. Indeed, this event properly orients the nitrogen lone pair toward Ser217 for the protonation and subsequent exit of the leaving group (Scheme 2). Although crucial in leading to the completeness of the catalytic function, the mechanistic details and the related energetic cost of this event remained unclear, leaving important questions about the effective role of nitrogen inversion in enzymatic activity unanswered. We are currently performing Car-Parrinello QM/MM simulations to clarify the role of this key event for amide bond hydrolysis of endogenous substrates in FAAH (Fig. 3).

Later, Mulholland et al. investigated the deacylation step of FAAH catalysis, with oleamide as a substrate covalently bound to Ser241, after hydrolysis (**D** → **E**) [118]. Based on the X-ray structures of FAAH covalently bound to the carbamoylating agents PF-3845 and URB597 [25], the authors corroborate the mechanistic hypothesis of a "deacylating water molecule" acting as a nucleophilic agent on the carbamoylated Ser241.

The essential role of flexibility of the protein/ligand complex for FAAH enzymatic activity and selectivity was also investigated by a more recent MD-based study from our group, which showed the key role of structural flexibility of the highly flexible substrate anandamide when in complex with FAAH [119]. We used microsecond MD simulations of FAAH embedded in a realistic membrane/water environment to show that anandamide may not lock itself into the AB cavity, but may rather assume catalytically significant conformations required for hydrolysis by moving its flexible arachidonoyl tail between the MA and AB cavities (Fig. 4, upper panel). This process is regulated by a phenylalanine residue (Phe432) located at the boundary between the two cavities, which may act as a "*dynamic paddle*" [21,45].

The location and conformational changes of anandamide during dynamics were identified and classified, together with conformational transitions of the amino acids located within the FAAH binding site (Phe381, Phe432 and Trp531). Also, the pre-organization of the FAAH active site for anandamide hydrolysis was identified via the definition of catalytically significant conformational states of the FAAH/anandamide complex. These are characterized by optimal distances and orientations of key

Please cite this article in press as: G. Palermo, et al., Computational insights into function and inhibition of fatty acid amide hydrolase, European Journal of Medicinal Chemistry (2014), http://dx.doi.org/10.1016/j.ejmech.2014.09.037

structural parameters involved in the enzymatic reaction, as described in a number of computational studies [29–32,120]. Using these descriptors, we found that anandamide reversibly moves its flexible arachidonoyl chain from the initial location in the MA channel into the AB channel (Fig. 4, upper panel). These MA ↔ AB transitions are triggered by the key residue Phe432 that, in tandem with the MA/AB interface residues Phe381 and Trp531, acts as a "*dynamic paddle*" and orients the substrates within the active site for hydrolysis, in agreement with what was previously suggested by Mileni et al. (Fig. 4, lower panel) [21].

Overall, our calculations suggest an essential role for substrate dynamics in facilitating the formation of catalytically significant conformations to attain FAAH activity, therefore suggesting a more dynamic scenario than that provided by the X-ray structure of FAAH in complex with the anandamide analog MAFP **(1)** [1]. Also, a recent work identified a possible pathway for substrate binding into FAAH from the membrane side [121]. Despite the absence of the transmembrane helices, the simulations further confirmed that the substrate enters into the active site via the enzymatic "membrane access" cavity, in agreement with previous results [27,119]. In FAAH, the interplay between the ligand and protein structural flexibility seems key to an understanding of the binding mechanism. This is supported by several other experimental data. In fact, crystallographic and biochemical studies have suggested that FAAH can adapt to the chemical nature of different lipid substrates or inhibitors thanks to a pronounced flexibility of its binding channels [21–26,45]. Accordingly, it is tempting to speculate that a similar mechanism might operate for other lipid amides that are hydrolyzed by FAAH, such as oleoylethanolamide and palmitoylethanolamide. FAAH controls the concentrations of these compounds in the brain via a distinct selection of the substrates that lead to the preferred anandamide hydrolysis [5,7]. Although the enzymatic activity of FAAH has been measured using different enzyme preparations and substrate analogues [5,7], the mechanistic bases of substrate selectivity remain unclear [3].

3.2. Covalent inhibition of FAAH

FAAH inhibition has been widely investigated via computational methods. Jorgensen et al. first clarified key aspects of the inhibition of FAAH by α-ketoheterocycle derivatives using MC simulations in conjunction with FEP calculations [28,113]. Mulholland et al. explored the reaction between FAAH and several carbamate-based inhibitors via QM/MM geometry optimizations (at the PM3[64]/CHARMM [75] level, corrected at DFT level), clarifying that these compounds inactivate FAAH by carbamoylation of the Ser241 nucleophile [39,40]. Recently, Mulholland et al. used QM/MM calculations to investigate the reactivation mechanism of FAAH carbamoylated by different covalent inhibitors [118]. They showed that the decarbamoylation process of FAAH covalent adducts is favored for the piperazinylurea JNJ1661610 (**10**) [41], with respect to the *O*-aryl carbamate URB597 **(6)** [37]. This finding is consistent with the experimental observation of a slowly reversible FAAH inhibition for the piperazinylurea inhibitor and irreversible inhibition for URB597 (**6**) [33,122].

In this scenario, we recently performed an extensive MD and QM/MM study on some relevant piperidine/piperazine urea-based compounds, providing insights into their mechanism for inhibiting FAAH [120]. We focused on the covalent agents PF-750 (**8** – piperidine-based) [42] and JNJ1661010 (**10** – piperazine-based) [41], which are two lead compounds used to generate clinical candidates (Scheme 3). These two potent compounds were compared to the inactive acyclic 1-cyclohexyl-3-naphthalen-2-ylurea ($IC_{50} \leq 30{,}000$ nM) [36] through the use of both MD simulations and QM/MM calculations. This comparative study highlighted a different conformational flexibility of these three representative compounds when in complex with FAAH and in water, supporting the previous hypothesis that FAAH is able to induce a distortion of the amide bond only when bound to piperidine and piperazine compounds, which are the effective inhibitors (Fig. 5, upper panel) [42]. MD simulations have indicated that, within FAAH's binding site, the piperidine and piperazine inhibitors assume specific conformations that are characterized by the twist of the amide bond and partial pyramidalization at the amide nitrogen. As a consequence of this amide bond distortion, the substrate is more prone to undergo nucleophilic attack by the catalytic Ser241, thereby facilitating enzyme inhibition through the formation of a covalent bond between the inhibitor and Ser241 [42].

These MD-based findings were corroborated using QM/MM calculations, which showed a higher reactivity of the distorted amides toward nucleophilic attack, relative to those of their planar analogues (Fig. 5, lower panel). We detected a more favorable HOMO–LUMO energy gap – calculated at the HF/6-311G**//AMBER99SB [123] level with the ONIOM method [124] – in the reactant state of the distorted amides of ~0.35–0.40 eV (i.e., ~8–9 kcal mol^{-1}), with respect to the planar analogues (Fig. 5). This result, coupled to a lack of distortion of the amide bond of the inactive compound during classical MD simulations, might explain the inability of planar compounds to inhibit FAAH. Overall, our study [120] supports the idea that the enzyme-induced twist of the amide bond likely facilitates amide bond hydrolysis and formation of the covalent inhibitor-enzyme adduct [42]. In contrast, the rigidity of the planar urea moiety in the acyclic derivative seems to prevent a good fit into the catalytic pocket, which might partially explain its lack of inhibitory activity. This rational explanation of the inhibitory mechanism of cyclic piperidine and piperazine aryl ureas agrees with results directly obtained with experiments [42], and could therefore be used as a simple indication of the propensity of new urea-based compounds to act as covalent inhibitors of FAAH. Ultimately, this is a further example of how MD and QM/MM methods, once prohibitive for practical drug design, have nowadays the potential to become a routine tool for drug design.

4. Conclusions

Here, we have reviewed several previous computational studies on catalysis and covalent inhibition of the enzyme FAAH. These have critically contributed to elucidating key aspects of the enzymatic mechanism of FAAH. A variety of computational approaches have been used in recent years to dissect both the function and inhibition of FAAH, spanning from classical molecular dynamics to full quantum mechanics and hybrid QM/MM methods. Mechanistic hypotheses on the mechanism for hydrolysis of either endogenous substrates or covalent inhibitors such as carbamates and piperidine/piperazine urea-based inhibitors have been computationally tested, providing model systems for the further design of better inhibitors. In addition, the role of structural flexibility for ligand binding has also been investigated by long time scale MD simulations. These investigations suggested that the interplay between the substrate and the protein structural flexibility is a key factor for substrate selection and catalytic activity of FAAH. This information could now be used to clarify, for example, crucial aspects related to the mechanism used by FAAH to select its principal substrate (i.e. anandamide) from among a complex cellular milieu of bioactive lipids. This question is thus far largely unanswered and could also be relevant for understanding fundamental principles for substrate selection in lipid-degrading enzymes.

Please cite this article in press as: G. Palermo, et al., Computational insights into function and inhibition of fatty acid amide hydrolase, European Journal of Medicinal Chemistry (2014), http://dx.doi.org/10.1016/j.ejmech.2014.09.037

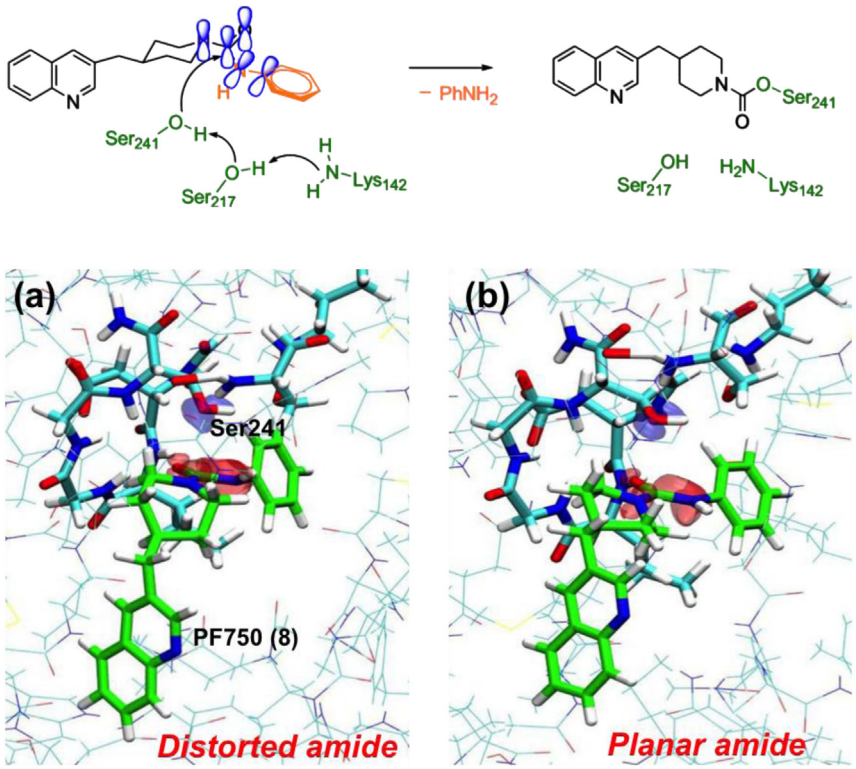

Fig. 5. Upper panel: Proposed mechanism of FAAH inhibition by the piperidine and piperazine ureas (shown for PF-750 – **8**) [42]. An enzyme-induced conformational change in the piperidine/piperazine scaffold weakens the conjugation of the nitrogen lone pair with the carbonyl, allowing a facile nucleophilic attack by Ser241. FAAH residues are colored green, while the leaving group is colored orange. Lower panel: Shape of the frontier orbitals for the *h*/*r*-FAAH/PF-750 complex [21]. Two representative snapshots from QM/MM calculations are shown, characterized by distorted (a) and planar (b) amide bonds. In (a), the LUMO orbital (red) is localized on the PF-750 carbonyl and is turned toward the HOMO orbital (blue) of the Ser241 nucleophile. In (b), the LUMO orbital is not centered on the electrophilic center of PF-750 and is therefore less prone to receiving the HOMO electron donor of the Ser241. A favored HOMO–LUMO energy gap of ~0.35–0.40 eV (i.e., ~8–9 kcal mol^{-1}) was calculated for the distorted amides (a), with respect to the planar analogues (b) [120]. Details are reported in the main text. The QM atoms of PF-750 (green) and of the protein residues (cyan) are shown in cyan, while the remaining part of the system, which has been treated at MM level, is shown with lines. (For interpretation of the references to color in this figure legend, the reader is referred to the web version of this article.)

Acknowledgments

MDV thanks the Italian Association for Cancer Research (AIRC) for the financial support through the "MFAG" Grant n. 14140. We also thank PRACE (Partnership for Advanced Computing in Europe) for HPC computing time.

Appendix A. Supplementary data

Supplementary data related to this article can be found at http://dx.doi.org/10.1016/j.ejmech.2014.09.037.

References

[1] M.H. Bracey, M.A. Hanson, K.R. Masuda, R.C. Stevens, B.F. Cravatt, Structural adaptations in a membrane enzyme that terminates endocannabinoid signaling, Science 298 (2002) 1793–1796.
[2] B.F. Cravatt, D.K. Giang, S.P. Mayfield, D.L. Boger, R.A. Lerner, N.B. Gilula, Molecular characterization of an enzyme that degrades neuromodulatory fatty-acid amides, Nature 384 (1996) 83–87.
[3] D. Piomelli, The molecular logic of endocannabinoid signalling, Nat. Rev. Neurosci. 4 (2003) 873–884.
[4] B.F. Cravatt, O. Prospero-Garcia, G. Siuzdak, N.B. Gilula, S.J. Henriksen, D.L. Boger, R.A. Lerner, Chemical characterization of a family of brain lipids that induce sleep, Science 268 (1995) 1506–1509.
[5] F. Desarnaud, H. Cadas, D. Piomelli, Anandamide amidohydrolase activity in rat brain microsomes. Identification and partial characterization, J. Biol. Chem. 270 (1995) 6030–6035.
[6] W.A. Devane, L. Hanus, A. Breuer, R.G. Pertwee, L.A. Stevenson, G. Griffin, D. Gibson, A. Mandelbaum, A. Etinger, R. Mechoulam, Isolation and structure of a brain constituent that binds to the cannabinoid receptor, Science 258 (1992) 1946–1949.
[7] D.L. Boger, R.A. Fecik, J.E. Patterson, H. Miyauchi, M.P. Patricelli, B.F. Cravatt, Fatty acid amide hydrolase substrate specificity, Bioorg. Med. Chem. Lett. 10 (2000) 2613–2616.
[8] G. Labar, C. Bauvois, F. Borel, J.L. Ferrer, J. Wouters, D.M. Lambert, Crystal structure of the human monoacylglycerol lipase, a key actor in endocannabinoid signaling, Chembiochem 11 (2010) 218–227.
[9] T. Sugiura, S. Kondo, A. Sukagawa, S. Nakane, A. Shinoda, K. Itoh, A. Yamashita, K. Waku, 2-Arachidonoylglycerol: a possible endogenous cannabinoid receptor ligand in brain, Biochem. Biophys. Res. Comm. 215 (1995) 89–97.
[10] P. Campolongo, B. Roozendaal, V. Trezza, V. Cuomo, G. Astarita, J. Fu, J.L. McGaugh, D. Piomelli, Fat-induced satiety factor oleoylethanolamide enhances memory consolidation, Proc. Natl. Acad. Sci. USA 106 (2009) 8027–8031.
[11] F. Rodriguez de Fonseca, M. Navarro, R. Gomez, L. Escuredo, F. Nava, J. Fu, E. Murillo-Rodriguez, A. Giuffrida, J. LoVerme, S. Gaetani, S. Kathuria, C. Gall, D. Piomelli, An anorexic lipid mediator regulated by feeding, Nature 414 (2001) 209–212.
[12] C. Solorzano, C. Zhu, N. Battista, G. Astarita, A. Lodola, S. Rivara, M. Mor, R. Russo, M. Maccarrone, F. Antonietti, A. Duranti, A. Tontini, S. Cuzzocrea, G. Tarzia, D. Piomelli, Selective N-acylethanolamine-hydrolyzing acid amidase inhibition reveals a key role for endogenous palmitoylethanolamide in inflammation, Proc. Natl. Acad. Sci. USA 106 (2009) 20966–20971.
[13] A. Makriyannis, 2012 division of medicinal chemistry award address. Trekking the cannabinoid road: a personal perspective, J. Med. Chem. 57 (2014) 3891–3911.
[14] B.F. Cravatt, K. Demarest, M.P. Patricelli, M.H. Bracey, D.K. Giang, B.R. Martin, A.H. Lichtman, Supersensitivity to anandamide and enhanced endogenous cannabinoid signaling in mice lacking fatty acid amide hydrolase, Proc. Natl. Acad. Sci. USA 98 (2001) 9371–9376.
[15] M. Karsak, E. Gaffal, R. Date, L. Wang-Eckhardt, J. Rehnelt, S. Petrosino, K. Starowicz, R. Steuder, E. Schlicker, B. Cravatt, R. Mechoulam, R. Buettner, S. Werner, V. Di Marzo, T. Tuting, A. Zimmer, Attenuation of allergic contact dermatitis through the endocannabinoid system, Science 316 (2007) 1494–1497.

[16] A.H. Lichtman, C.C. Shelton, T. Advani, B.F. Cravatt, Mice lacking fatty acid amide hydrolase exhibit a cannabinoid receptor-mediated phenotypic hypoalgesia, Pain 109 (2004) 319–327.
[17] K. Otrubova, M. Brown, M.S. McCormick, G.W. Han, S.T. O'Neal, B.F. Cravatt, R.C. Stevens, A.H. Lichtman, D.L. Boger, Rational design of fatty acid amide hydrolase inhibitors that act by covalently bonding to two active site residues, J. Am. Chem. Soc. 135 (2013) 6289–6299.
[18] L. Bertolacci, E. Romeo, M. Veronesi, P. Magotti, C. Albani, M. Dionisi, C. Lambruschini, R. Scarpelli, A. Cavalli, M. De Vivo, D. Piomelli, G. Garau, A binding site for nonsteroidal anti-inflammatory drugs in fatty acid amide hydrolase, J. Am. Chem. Soc. 135 (2013) 22–25.
[19] A.D. Favia, D. Habrant, R. Scarpelli, M. Migliore, C. Albani, S.M. Bertozzi, M. Dionisi, G. Tarozzo, D. Piomelli, A. Cavalli, M. De Vivo, Identification and characterization of carprofen as a multitarget fatty acid amide hydrolase/cyclooxygenase inhibitor, J. Med. Chem. 55 (2012) 8807–8826.
[20] M.P. Patricelli, H.A. Lashuel, D.K. Giang, J.W. Kelly, B.F. Cravatt, Comparative characterization of a wild type and transmembrane domain-deleted fatty acid amide hydrolase: identification of the transmembrane domain as a site for oligomerization, Biochemistry 37 (1998) 15177–15187.
[21] M. Mileni, D.S. Johnson, Z. Wang, D.S. Everdeen, M. Liimatta, B. Pabst, K. Bhattacharya, R.A. Nugent, S. Kamtekar, B.F. Cravatt, K. Ahn, R.C. Stevens, Structure-guided inhibitor design for human FAAH by interspecies active site conversion, Proc. Natl. Acad. Sci. USA 105 (2008) 12820–12824.
[22] K. Ahn, D.S. Johnson, M. Mileni, D. Beidler, J.Z. Long, M.K. McKinney, E. Weerapana, N. Sadagopan, M. Liimatta, S.E. Smith, S. Lazerwith, C. Stiff, S. Kamtekar, K. Bhattacharya, Y. Zhang, S. Swaney, K. Van Becelaere, R.C. Stevens, B.F. Cravatt, Discovery and characterization of a highly selective FAAH inhibitor that reduces inflammatory pain, Chem. Biol. 16 (2009) 411–420.
[23] M. Mileni, J. Garfunkle, J.K. DeMartino, B.F. Cravatt, D.L. Boger, R.C. Stevens, Binding and inactivation mechanism of a humanized fatty acid amide hydrolase by alpha-ketoheterocycle inhibitors revealed from cocrystal structures, J. Am. Chem. Soc. 131 (2009) 10497–10506.
[24] M. Mileni, J. Garfunkle, C. Ezzili, F.S. Kimball, B.F. Cravatt, R.C. Stevens, D.L. Boger, X-ray crystallographic analysis of alpha-ketoheterocycle inhibitors bound to a humanized variant of fatty acid amide hydrolase, J. Med. Chem. 53 (2010) 230–240.
[25] M. Mileni, S. Kamtekar, D.C. Wood, T.E. Benson, B.F. Cravatt, R.C. Stevens, Crystal structure of fatty acid amide hydrolase bound to the carbamate inhibitor URB597: discovery of a deacylating water molecule and insight into enzyme inactivation, J. Mol. Biol. 400 (2010) 743–754.
[26] X. Min, S.T. Thibault, A.C. Porter, D.J. Gustin, T.J. Carlson, H. Xu, M. Lindstrom, G. Xu, C. Uyeda, Z. Ma, Y. Li, F. Kayser, N.P. Walker, Z. Wang, Discovery and molecular basis of potent noncovalent inhibitors of fatty acid amide hydrolase (FAAH), Proc. Natl. Acad. Sci. USA 108 (2011) 7379–7384.
[27] M.K. McKinney, B.F. Cravatt, Evidence for distinct roles in catalysis for residues of the serine-serine-lysine catalytic triad of fatty acid amide hydrolase, J. Biol. Chem. 278 (2003) 37393–37399.
[28] C.R. Guimaraes, D.L. Boger, W.L. Jorgensen, Elucidation of fatty acid amide hydrolase inhibition by potent alpha-ketoheterocycle derivatives from Monte Carlo simulations, J. Am. Chem. Soc. 127 (2005) 17377–17384.
[29] A. Lodola, M. Mor, J.C. Hermann, G. Tarzia, D. Piomelli, A.J. Mulholland, QM/MM modelling of oleamide hydrolysis in fatty acid amide hydrolase (FAAH) reveals a new mechanism of nucleophile activation, Chem. Commun. (Camb) (2005) 4399–4401.
[30] A. Lodola, M. Mor, J. Zurek, G. Tarzia, D. Piomelli, J.N. Harvey, A.J. Mulholland, Conformational effects in enzyme catalysis: reaction via a high energy conformation in fatty acid amide hydrolase, Biophys. J. 15 (2006) L20–L22.
[31] A. Lodola, J. Sirirak, N. Fey, S. Rivara, M. Mor, A.J. Mulholland, Structural fluctuations in enzyme-catalyzed reactions: determinants of reactivity in fatty acid amide hydrolase from multivariate statistical analysis of quantum mechanics/molecular mechanics paths, J. Chem. Theory Comput. 6 (2010) 2948–2960.
[32] I. Tubert-Brohman, O. Acevedo, W.L. Jorgensen, Elucidation of hydrolysis mechanisms for fatty acid amide hydrolase and its Lys142Ala variant via QM/MM simulations, J. Am. Chem. Soc. 128 (2006) 16904–16913.
[33] M. Seierstad, J.G. Breitenbucher, Discovery and development of fatty acid amide hydrolase (FAAH) inhibitors, J. Med. Chem. 51 (2008) 7327–7343.
[34] C. Ezzili, M. Mileni, N. McGlinchey, J.Z. Long, S.G. Kinsey, D.G. Hochstatter, R.C. Stevens, A.H. Lichtman, B.F. Cravatt, E.J. Bilsky, D.L. Boger, Reversible competitive alpha-ketoheterocycle inhibitors of fatty acid amide hydrolase containing additional conformational constraints in the acyl side chain: orally active, long-acting analgesics, J. Med. Chem. 54 (2011) 2805–2822.
[35] S. Kathuria, S. Gaetani, D. Fegley, F. Valino, A. Duranti, A. Tontini, M. Mor, G. Tarzia, G. La Rana, A. Calignano, A. Giustino, M. Tattoli, M. Palmery, V. Cuomo, D. Piomelli, Modulation of anxiety through blockade of anandamide hydrolysis, Nat. Med. 9 (2003) 76–81.
[36] G. Tarzia, A. Duranti, A. Tontini, G. Piersanti, M. Mor, S. Rivara, P.V. Plazzi, C. Park, S. Kathuria, D. Piomelli, Design, synthesis, and structure-activity relationships of alkylcarbamic acid aryl esters, a new class of fatty acid amide hydrolase inhibitors, J. Med. Chem. 46 (2003) 2352–2360.
[37] M. Mor, S. Rivara, A. Lodola, P.V. Plazzi, G. Tarzia, A. Duranti, A. Tontini, G. Piersanti, S. Kathuria, D. Piomelli, Cyclohexylcarbamic acid 3'- or 4'-substituted biphenyl-3-yl esters as fatty acid amide hydrolase inhibitors: synthesis, quantitative structure-activity relationships, and molecular modeling studies, J. Med. Chem. 47 (2004) 4998–5008.
[38] J.R. Clapper, G. Moreno-Sanz, R. Russo, A. Guijarro, F. Vacondio, A. Duranti, A. Tontini, S. Sanchini, N.R. Sciolino, J.M. Spradley, A.G. Hohmann, A. Calignano, M. Mor, G. Tarzia, D. Piomelli, Anandamide suppresses pain initiation through a peripheral endocannabinoid mechanism, Nat. Neurosci. 13 (2010) 1265–1270.
[39] A. Lodola, L. Capoferri, S. Rivara, E. Chudyk, J. Sirirak, E. Dyguda-Kazimierowicz, W. Andrzej Sokalski, M. Mileni, G. Tarzia, D. Piomelli, M. Mor, A.J. Mulholland, Understanding the role of carbamate reactivity in fatty acid amide hydrolase inhibition by QM/MM mechanistic modelling, Chem. Commun. (Camb) 47 (2011) 2517–2519.
[40] A. Lodola, M. Mor, S. Rivara, C. Christov, G. Tarzia, D. Piomelli, A.J. Mulholland, Identification of productive inhibitor binding orientation in fatty acid amide hydrolase (FAAH) by QM/MM mechanistic modelling, Chem. Commun. (Camb) (2008) 214–216.
[41] J.M. Keith, R. Apodaca, W. Xiao, M. Seierstad, K. Pattabiraman, J. Wu, M. Webb, M.J. Karbarz, S. Brown, S. Wilson, B. Scott, C.S. Tham, L. Luo, J. Palmer, M. Wennerholm, S. Chaplan, J.G. Breitenbucher, Thiadiazolopiperazinyl ureas as inhibitors of fatty acid amide hydrolase, Bioorg. Med. Chem. Lett. 18 (2008) 4343–4838.
[42] K. Ahn, D.S. Johnson, L.R. Fitzgerald, M. Liimatta, A. Arendse, T. Stevenson, E.T. Lund, R.A. Nugent, T.K. Nomanbhoy, J.P. Alexander, B.F. Cravatt, Novel mechanistic class of fatty acid amide hydrolase inhibitors with remarkable selectivity, Biochemistry 46 (2007) 13019–13030.
[43] M.K. McKinney, B.F. Cravatt, Structure and function of fatty acid amide hydrolase, Annu. Rev. Biochem 74 (2005) 411–432.
[44] K. Ahn, D.S. Johnson, B.F. Cravatt, Fatty acid amide hydrolase as a potential therapeutic target for the treatment of pain and CNS disorders, Expert Opin. Drug. Discov. 4 (2009) 763–784.
[45] G. Mei, A. Di Venere, V. Gasperi, E. Nicolai, K.R. Masuda, A. Finazzi-Agro, B.F. Cravatt, M. Maccarrone, Closing the gate to the active site: effect of the inhibitor methoxyarachidonyl fluorophosphonate on the conformation and membrane binding of fatty acid amide hydrolase, J. Biol. Chem. 282 (2007) 3829–3836.
[46] C. Moller, M.S. Plesset, Note on an approximation treatment for many-electron systems, Phys. Rev. 46 (1934) 0618–0622.
[47] P. Hohenberg, W. Kohn, In homogeneous electron gas, Phys. Rev. B 136 (1964) B864.
[48] W. Kohn, L.J. Sham, Self-consistent equations including exchange and correlation effects, Phys. Rev. 140 (1965) 1133.
[49] A.D. Becke, Density-functional exchange-energy approximation with correct asymptotic-behavior, Phys. Rev. A 38 (1988) 3098–3100.
[50] C.T. Lee, W.T. Yang, R.G. Parr, Development of the Colle-Salvetti correlation-energy formula into a functional of the electron-density, Phys. Rev. B 37 (1988) 785–789.
[51] A.D. Becke, A new mixing of Hartree-Fock and local density-functional theories, J. Chem. Phys. 98 (1993) 1372–1377.
[52] S.H. Vosko, L. Wilk, M. Nusair, Accurate spin-dependent electron liquid correlation energies for local spin-density calculations – a critical analysis, Can. J. Phys. 58 (1980) 1200–1211.
[53] P. Carloni, U. Rothlisberger, M. Parrinello, The role and perspective of ab initio molecular dynamics in the study of biological systems, Acc. Chem. Res. 35 (2002) 455–464.
[54] U. Rothlisberger, P. Carloni, Drug-target binding investigated by quantum mechanical/molecular mechanical (QM/MM), Methods. Lect. Notes Phys. 704 (2006) 449–479.
[55] Y. Zhao, D.G. Truhlar, Density functionals with broad applicability in chemistry, Acc. Chem. Res. 41 (2008) 157–167.
[56] Y. Zhao, D.G. Truhlar, The M06 suite of density functionals for main group thermochemistry, thermochemical kinetics, noncovalent interactions, excited states, and transition elements: two new functionals and systematic testing of four M06-class functionals and 12 other functionals, Theor. Chem. Acc. 120 (2008) 215–241.
[57] R. Car, M. Parrinello, Unified approach for molecular-dynamics and density-functional theory, Phys. Rev. Lett. 55 (1985) 2471–2474.
[58] E. Brunk, N. Ashari, P. Athri, P. Campomanes, F.F. de Carvalho, B.F.E. Curchod, P. Diamantis, M. Doemer, J. Garrec, A. Laktionov, M. Micciarelli, M. Neri, G. Palermo, T.J. Penfold, S. Vanni, I. Tavernelli, U. Rothlisberger, Pushing the frontiers of first-principles based computer simulations of chemical and biological systems, Chimia 65 (2011) 667–671.
[59] M. Dal Peraro, A.J. Vila, P. Carloni, M.L. Klein, Role of zinc content on the catalytic efficiency of B1 metallo beta-lactamases, J. Am. Chem. Soc. 129 (2007) 2808–2816.
[60] M. De Vivo, M. Dal Peraro, M.L. Klein, Phosphodiester cleavage in ribonuclease H occurs via an associative two-metal-aided catalytic mechanism, J. Am. Chem. Soc. 130 (2008) 10955–10962.
[61] M. De Vivo, B. Ensing, M. Dal Peraro, G.A. Gomez, D.W. Christianson, M.L. Klein, Proton shuttles and phosphatase activity in soluble epoxide hydrolase, J. Am. Chem. Soc. 129 (2007) 387–394.
[62] M. De Vivo, B. Ensing, M.L. Klein, Computational study of phosphatase activity in soluble epoxyde hydrolase: high efficiency through a water bridge mediated proton shuttle, J. Am. Chem. Soc. 127 (32) (2005) 11226–11227.
[63] M.J.S. Dewar, W. Thiel, Ground-states of molecules. 38. Mndo method – approximations and parameters, J. Am. Chem. Soc. 99 (1977) 4899–4907.

Please cite this article in press as: G. Palermo, et al., Computational insights into function and inhibition of fatty acid amide hydrolase, European Journal of Medicinal Chemistry (2014), http://dx.doi.org/10.1016/j.ejmech.2014.09.037

[64] M.J.S. Dewar, D.M. Storch, The development and use of quantum molecular-models. 75. Comparative tests of theoretical procedures for studying chemical-reactions, J. Am. Chem. Soc. 107 (1985) 3898–3902.
[65] J.J.P. Stewart, Optimization of parameters for semiempirical methods .1, Method. J. Comput. Chem. 10 (1989) 209–220.
[66] M.P. Repasky, J. Chandrasekhar, W.L. Jorgensen, PDDG/PM3 and PDDG/MNDO: Improved semiempirical methods, J. Comput. Chem. 23 (2002) 1601–1622.
[67] B.J. Alder, T.E. Wainwright, Phase transition for a hard sphere system, J. Chem. Phys. 27 (1957) 1208–1209.
[68] E. Fermi, J.G. Pasta, S.M. Ulam, Los Alamos LASL Report, 1955.
[69] A. Rahman, Correlations in the motion of atoms in liquid argon, Phys. Rev. A 136 (1964) 405–411.
[70] M.P. Allen, D.J. Tildesley, Computer Simulation of Liquids, second ed., Oxford University Press, Oxford, 1994.
[71] D. Frenkel, B. Smit, Understanding Molecular Simulation, second ed., Academic Press, San Diego, 2002.
[72] W.L. Jorgensen, D.S. Maxwell, J. Tirado-Rives, Development and testing of the OPLS all-atom force field on conformational energetics and properties of organic liquids, J. Am. Chem. Soc. 118 (1996) 11225–11236.
[73] Y. Duan, C. Wu, S. Chowdhury, M.C. Lee, G. Xiong, W. Zhang, R. Yang, P. Cieplak, R. Luo, T. Lee, J. Caldwell, J. Wang, P. Kollman, A point-charge force field for molecular mechanics simulations of proteins based on condensed-phase quantum mechanical calculations, J. Comput. Chem. 24 (2003) 1999–2012.
[74] M. Christen, P.H. Hunenberger, D. Bakowies, R. Baron, R. Burgi, D.P. Geerke, T.N. Heinz, M.A. Kastenholz, V. Krautler, C. Oostenbrink, C. Peter, D. Trzesniak, W.F. van Gunsteren, The GROMOS software for biomolecular simulation: GROMOS05, J. Comput. Chem. 26 (2005) 1719–1751.
[75] A.D. MacKerell, D.J. Bashford, M. Bellott, R.L. Dunbrack, D.J.J. Evanseck, J.M. Field, S. Fischer, J. Gao, H. Guo, S. Ha, D. Joseph-McCarthy, L. Kuchnir, K. Kuczera, K.T.F. Lau, C. Mattos, S. Michnick, T. Ngo, D.T. Nguyen, B. Prodhom, E.W. Reiher, B.I. Roux, M. Schlenkrich, J.C. Smith, R. Stote, J. Straub, M. Watanabe, J. Wiorkiewicz-Kuczera, D. Yin, M. Karplus, All-Atom empirical potential for molecular modeling and dynamics studies of proteins, Phys. Chem. B 102 (1998) 3586–3616.
[76] J. Wang, R.M. Wolf, J.W. Caldwell, P.A. Kollman, D.A. Case, Development and testing of a general amber force field, J. Comput. Chem. 25 (2004) 1157–1174.
[77] K. Vanommeslaeghe, E. Hatcher, C. Acharya, S. Kundu, S. Zhong, J. Shim, E. Darian, O. Guvench, P. Lopes, I. Vorobyov, A.D. Mackerell Jr., CHARMM general force field: a force field for drug-like molecules compatible with the CHARMM all-atom additive biological force fields, J. Comput. Chem. 31 (2010) 671–690.
[78] M. De Vivo, A. Cavalli, G. Bottegoni, P. Carloni, M. Recanatini, Role of phosphorylated Thr160 for the activation of the CDK2/Cyclin a complex, Proteins Struct. Funct. Bioinform. 62 (2006) 89–98.
[79] M. De Vivo, G. Bottegoni, A. Berteotti, M. Recanatini, F.L. Gervasio, A. Cavalli, Cyclin-dependent kinases: bridging their structure and function through computations, Future Med. Chem. 3 (2011) 1551–1559.
[80] A. Laio, M. Parrinello, Escaping free-energy minima, Proc. Natl. Acad. Sci. USA 99 (2002) 12562–12566.
[81] B. Ensing, M. De Vivo, Z.W. Liu, P. Moore, M.L. Klein, Metadynamics as a tool for exploring free energy landscapes of chemical reactions, Acc. Chem. Res. 39 (2006) 73–81.
[82] W.L. Jorgensen, Efficient drug lead discovery and optimization, Acc. Chem. Res. 42 (2009) 724–733.
[83] W.L. Jorgensen, L.L. Thomas, Perspective on free-energy perturbation calculations for chemical equilibria, J. Chem. Theory Comput. 4 (2004) 869–876.
[84] I. Bisha, A. Laio, A. Magistrato, A. Giorgetti, J. Sgrignani, A candidate ion-retaining state in the inward-facing conformation of sodium/galactose symporter: clues from atomistic simulations, J. Chem. Theory Comput. 9 (2013) 1240–1246.
[85] A. Warshel, M. Levitt, Theoretical studies of enzymic reactions: dielectric, electrostatic and steric stabilization of the carbonium ion in the reaction of lysozyme, J. Mol. Biol. 103 (1976) 227–249.
[86] R.A. Friesner, V. Guallar, Ab initio quantum chemical and mixed quantum mechanics/molecular mechanics (QM/MM) methods for studying enzymatic catalysis, Annu. Rev. Phys. Chem. 56 (2005) 389–427.
[87] H.M. Senn, W. Thiel, QM/MM methods for biomolecular systems, Angew. Chem. Int. Ed. Engl. 48 (2009) 1198–1229.
[88] A. Warshel, Computer simulations of enzyme catalysis: methods, progress, and insights, Ann. Rev. Biophys. Biomolec. Struct. 32 (2003) 425–443.
[89] J.L. Gao, Hybrid quantum and molecular mechanical simulations: an alternative avenue to solvent effects in organic chemistry, Acc. Chem. Res. 29 (1996) 298–305.
[90] A. Cavalli, P. Carloni, M. Recanatini, Target-related applications of first principles quantum chemical methods in drug design, Chem. Rev. 106 (2006) 3497–3519.
[91] M. Dal Peraro, P. Ruggerone, S. Raugei, F.L. Gervasio, P. Carloni, Investigating biological systems using first principles Car-Parrinello molecular dynamics simulations, Curr. Opin. Struct. Biol. 17 (2007) 149–156.
[92] T. Vreven, K.S. Byun, I. Komaromi, S. Dapprich, J.A. Montgomery, K. Morokuma, M.J. Frisch, Combining quantum mechanics methods with molecular mechanics methods in ONIOM, J. Chem. Theory. Comput. 2 (2006) 815–826.
[93] G.W. Trucks, H.B. Schlegel, G.E. Scuseria, M.A. Robb, J.R. Cheeseman, G. Scalmani, V. Barone, B. Mennucci, G.A. Petersson, H. Nakatsuji, M. Caricato, X. Li, H.P. Hratchian, A.F. Izmaylov, J. Bloino, G. Zheng, J.L. Sonnenberg, M. Hada, M. Ehara, K. Toyota, R. Fukuda, J. Hasegawa, M. Ishida, T. Nakajima, Y. Honda, O. Kitao, H. Nakai, T., J.A. Montgomery Jr., J.E. Peralta, F. Ogliaro, M. Bearpark, J.J. Heyd, E. Brothers, K.N. Kudin, V.N. Staroverov, R. Kobayashi, J. Normand, K. Raghavachari, A. Rendell, J.C. Burant, S.S. Iyengar, J. Tomasi, M. Cossi, N. Rega, J.M. Millam, M. Klene, J.E. Knox, J.B. Cross, V. Bakken, C. Adamo, J. Jaramillo, R. Gomperts, R.E. Stratmann, O. Yazyev, A.J. Austin, R. Cammi, C. Pomelli, J.W. Ochterski, R.L. Martin, K. Morokuma, V.G. Zakrzewski, G.A. Voth, P. Salvador, J.J. Dannenberg, S. Dapprich, A.D. Daniels, Ö. Farkas, J.B. Foresman, J.V. Ortiz, J. Cioslowski, D.J. Fox, Gaussian 09, M. J. F., Gaussian, Inc, Wallingford CT, 2009.
[94] A. Laio, J. VandeVondele, U. Rothlisberger, D-RESP: dynamically generated electrostatic potential derived charges from quantum mechanics/molecular mechanics simulations, J. Phys. Chem. B 106 (2002) 7300–7307.
[95] A. Laio, J. VandeVondele, U. Rothlisberger, A Hamiltonian electrostatic coupling scheme for hybrid Car-Parrinello molecular dynamics simulations, J. Chem. Phys. 116 (2002) 6941–6947.
[96] T. Laino, F. Mohamed, A. Laio, M. Parrinello, An efficient real space multigrid OM/MM electrostatic coupling, J. Chem. Theory. Comput. 1 (2005) 1176–1184.
[97] R.A. Friesner, Combined quantum and molecular mechanics (QM/MM), Drug. Discov. Today: Technol. 1 (2004) 253–260.
[98] M.P. Gleeson, D. Gleeson, QM/MM calculations in drug discovery: a useful method for studying binding Phenomena? J. Chem. Inf. Model 49 (2009) 670–677.
[99] M.P. Gleeson, D. Gleeson, QM/MM as a tool in fragment based drug discovery. A cross-docking, rescoring study of kinase inhibitors, J. Chem. Inf. Model 49 (2009) 1437–1448.
[100] A. Lodola, M. De Vivo, The increasing role of QM/MM in drug discovery, Adv. Protein Chem. Struct. Biol. 87 (2012) 337–362.
[101] M. De Vivo, Bridging quantum mechanics and structure-based drug design, Front. Biosci. Landmrk 16 (2011) 1619–1633.
[102] A. Lodola, D. Branduardi, M. De Vivo, L. Capoferri, M. Mor, D. Piomelli, A. Cavalli, A catalytic mechanism for cysteine N-terminal nucleophile hydrolases, as revealed by free energy simulations, PLoS One 7 (2012) e32397.
[103] F. Claeyssens, J.N. Harvey, F.R. Manby, R.A. Mata, A.J. Mulholland, K.E. Ranaghan, M. Schutz, S. Thiel, W. Thiel, H.J. Werner, High-accuracy computation of reaction barriers in enzymes, Angew. Chem. Int. Ed. Engl. 45 (2006) 6856–6859.
[104] A.J. Mulholland, Computational enzymology: modelling the mechanisms of biological catalysts, Biochem. Soc. Trans. 36 (2008) 22–26.
[105] E. Rosta, M. Klahn, A. Warshel, Towards accurate ab initio QM/MM calculations of free-energy profiles of enzymatic reactions, J. Phys. Chem. B 110 (2006) 2934–2941.
[106] M.H. Ho, M. De Vivo, M. Dal Peraro, M.L. Klein, Unraveling the catalytic pathway of metalloenzyme farnesyltransferase through QM/MM computation, J. Chem. Theory Comput. 5 (2009) 1657–1666.
[107] G. Palermo, M. Stenta, A. Cavalli, M. Dal Peraro, M. De Vivo, Molecular simulations highlight the role of metals in catalysis and inhibition of type II topoisomerase, J. Chem. Theory Comput. 9 (2013) 857–862.
[108] A.E. Cho, V. Guallar, B.J. Berne, R. Friesner, Importance of accurate charges in molecular docking: quantum mechanical/molecular mechanical (QM/MM) approach, Comput. Chem. 26 (2005) 915–931.
[109] A. Khandelwal, V. Lukacova, D. Comez, D.M. Kroll, S. Raha, S. Balaz, A combination of docking, QM/MM methods, and MD simulation for binding affinity estimation of metalloprotein ligands, J. Med. Chem. 48 (2005) 5437–5447.
[110] T. Sander, T. Lijefors, T. Balle, Prediction of the receptor conformation for iGluR2 agonist binding: QM/MM docking to an extensive conformational ensemble generated using normal mode analysis, J. Mol. Graph. Model 26 (2008) 1259–1268.
[111] M. Kaukonen, P. Soderhjelm, J. Heimdal, U. Ryde, QM/MM-PBSA method to estimate free energies for reactions in proteins, J. Phys. Chem. B 112 (2008) 12537–12548.
[112] A. Khandelwal, S. Balaz, QM/MM linear response method distinguishes ligand affinities for closely related metalloproteins, Protein – Struct. Funct. Bioinforma. 69 (2007) 326–339.
[113] D.L. Boger, H. Miyauchi, W. Du, C. Hardouin, R.A. Fecik, H. Cheng, I. Hwang, M.P. Hedrick, D. Leung, O. Acevedo, C.R. Guimaraes, W.L. Jorgensen, B.F. Cravatt, Discovery of a potent, selective, and efficacious class of reversible alpha-ketoheterocycle inhibitors of fatty acid amide hydrolase effective as analgesics, J. Med. Chem. 48 (2005) 1849–1856.
[114] L. Capoferri, M. Mor, J. Sirirak, E. Chudyk, A.J. Mulholland, A. Lodola, Application of a SCC-DFTB QM/MM approach to the investigation of the catalytic mechanism of fatty acid amide hydrolase, J. Mol. Model 17 (2011) 2375–2383.
[115] A. Lodola, M. Mor, J. Sirirak, A.J. Mulholland, Insights into the mechanism and inhibition of fatty acid amide hydrolase from quantum mechanics/molecular mechanics (QM/MM) modelling, Biochem. Soc. Trans. 37 (2009) 363–367.
[116] J. Gao, S. Ma, D.T. Major, K. Nam, J. Pu, D.G. Truhlar, Mechanisms and free energies of enzymatic reactions, Chem. Rev. 16 (2006) 3188–3209.

Please cite this article in press as: G. Palermo, et al., Computational insights into function and inhibition of fatty acid amide hydrolase, European Journal of Medicinal Chemistry (2014), http://dx.doi.org/10.1016/j.ejmech.2014.09.037

[117] O. Acevedo, W.L. Jorgensen, Advances in quantum and molecular mechanical (QM/MM) simulations for organic and enzymatic reactions, Acc. Chem. Res. 43 (2010) 142–151.
[118] A. Lodola, L. Capoferri, S. Rivara, G. Tarzia, D. Piomelli, A. Mulholland, M. Mor, Quantum mechanics/molecular mechanics modeling of fatty acid amide hydrolase reactivation distinguishes substrate from irreversible covalent inhibitors, J. Med. Chem. 56 (2013) 2500–2512.
[119] G. Palermo, P. Campomanes, M. Neri, D. Piomelli, A. Cavalli, U. Rothlisberger, M. De Vivo, Wagging the tail: essential role of substrate flexibility in FAAH catalysis, J. Chem. Theory Comput. 9 (2013) 1202–1213.
[120] G. Palermo, D. Branduardi, M. Masetti, A. Lodola, M. Mor, D. Piomelli, A. Cavalli, M. De Vivo, Covalent inhibitors of fatty acid amide hydrolase: a rationale for the activity of piperidine and piperazine aryl ureas, J. Med. Chem. 54 (2011) 6612–6623.
[121] E. Dainese, G. De Fabritiis, A. Sabatucci, S. Oddi, C.B. Angelucci, C. Di Pancrazio, T. Giorgino, N. Stanley, M. Del Carlo, B.F. Cravatt, M. Maccarrone, Membrane lipids are key modulators of the endocannabinoid-hydrolase FAAH, Biochem. J. 457 (2014) 463–472.
[122] M.J. Karbarz, L. Luo, L. Chang, C.S. Tham, J.A. Palmer, S.J. Wilson, M.L. Wennerholm, S.M. Brown, B.P. Scott, R.L. Apodaca, J.M. Keith, J. Wu, J.G. Breitenbucher, S.R. Chaplan, M. Webb, Biochemical and biological properties of 4-[3-phenyl-[1,2,4] thiadiazol-5-yl]-piperazine-1-carboxylic acid phenylamide, a mechanism-based inhibitor of fatty acid amide hydrolase, Anesth. Analgesia 108 (2009) 316–329.
[123] V. Hornak, R. Abel, A. Okur, B. Strockbine, A. Roitberg, C. Simmerling, Comparison of multiple Amber force fields and development of improved protein backbone parameters, Proteins 65 (2006) 712–725.
[124] T. Vreven, K. Morokuma, O. Farkas, H.B. Schlegel, M.J. Frisch, Geometry optimization with QM/MM, ONIOM, and other combined methods. I. Microiterations and constraints, J. Comput. Chem. 24 (2003) 760–769.

Please cite this article in press as: G. Palermo, et al., Computational insights into function and inhibition of fatty acid amide hydrolase, European Journal of Medicinal Chemistry (2014), http://dx.doi.org/10.1016/j.ejmech.2014.09.037